CHEMICAL ENGINEERING TRANSACTIONS
VOL. 68, 2018
A publication of AIDIC
The Italian Association of Chemical Engineering
Online at www.aidic.it/cet
Guest Editors: Selena Sironi, Laura Capelli

ISBN 978-88-95608-65-5; **ISSN** 2283-9216
DOI: 10.3303/CET1868020

Special Odor Source Localization Based on Internet of Mobile Things

Changyi Jiao

Hebi Polytechnic, Hebi 458030, China
78308908@qq.com

Odor is closely bound up with people's lives. Hazardous gases can do us more harm. It is now imperative to take a deep dive into life odors in order to lessen the harm the hazardous gases cause to human body. In modern times, the integration of mobile internet and odor source localization is a new trend of current study in the field. A plume model is used herein to conduct a simulation experiment on odor source localization based on the IoMT (Internet of Mobile Things). Study results show that: indoor simulation experiment has a very high success rate, but there is a fuzzy effect of the step size and the sensor distribution radius on the success rate of the odor source localization; if the step size and the sensor distribution radius are lesser, the success rate of the odor source localization is subjected to the two to a certain extent and shows a downward trend. The success rate of simulation experiment in the outdoor environment is significantly lower than that in the indoor environment. Therefore, it is very important to choose a reasonable range of values in the simulation experiment.

1. Introduction

Odor has a direct bearing on people's lives. There are some gases in the air, which can cause great harm to human body. In this case, it is imperative for us to probe into the odors in order to lessen the harm done by these gases to human body (Li et al., 2011). The Internet of Things (IoT) is integrated with the Internet via a number of small sense networks to fully grasp the intranet information communication, thus enabling individual trace, location and surveillance (Lu et al., 2014). A hotspot in current study is to integrate the IoMT and odor source localization, so that the study of odor source localization based on the IoMT is bound to have a broad application prospects in the fields of tracing hazardous gases and fire preventing (Esquivelzeta et al., 2017).
The study of the odor source localization mainly originated from the 1980s. Many experts and scholars at home and abroad had made extensive studies on odor source localization at that time, and their efforts have borne productive fruits. Some scholars used robots to simulate the location of odor sources (Sato et al., 2010; Saxena et al., 2018); some applied fluid mechanics and stochastic process theory to the odor source localization (Ishida et al., 2006; Kowadlo and Russell, 2006; Gardiner and Atema, 2007), and some also introduced the visual localization for exploring it (Pyk et al., 2006; Frye et al., 2003). This paper, based on the IoMT, conducts a simulation experiment with a smoke plume model to dive into the odor source location, so that it has a strong practical application value.

2. Basic theory of plume model

The trajectory path formed by the diffusion of gas molecules in the air is called plume. As the impact of air torrent cannot be predicted more accurately, the plume structure seems more complicated and the distribution is uneven (Sumner, 2006). There are two types of plume model, i.e. static and dynamic models. In general, static model is used to track odor sources, while dynamic model is mainly used in simulation experiments.

2.1 Static model

There are two types of static plume models, i.e. Gaussian and BM models. The assumptions that need to be met in the application process are given as follows: no obstacles in the space, the wind speed remains unchanged; the wind is in the positive direction of the x-axis; there is only one odor source, located at (x_s, y_s);

Please cite this article as: Jiao C., 2018, Special odor source localization based on internet of mobile things, Chemical Engineering Transactions, 68, 115-120 DOI: 10.3303/CET1868020

the release rate q of the odor source remains unchanged (Agassounon et al., 2004). The gas concentration value is obtained by the formula:

$$C(x_i, y_i) = \frac{q}{2\pi K}\frac{1}{x_i} exp\left[-\frac{U}{2K}(d - (x_i - x_s))\right] \quad (1)$$

Where (x_i, y_i) is the sensor coordinate; $C(x_i, y_i)$ is the concentration value of the sensor at (x_i, y_i); d is the distance from the sensor to the odor source. The calculation formula is:

$$d = \sqrt{(x_i - x_s)^2 + (y_i - y_s)^2} \quad (2)$$

The static plume model effectively simplifies externally complex environment information. It is often used in the estimation process, but in general, it cannot simulate more complex experiment environments (Goken et al., 2010).

2.2 Dynamic model

Currently, the most widely used dynamic plume model is the atmospheric diffusion plume model. Odor source releases puffs mainly composed of countless filaments which constitute a gas plume. Impacted by different scales of vortices in the vortex, the filaments take on many forms of motion (Lu et al., 2013). If the filament is smaller than the vortex, it, as a whole, will present a convective motion, expressed as v_a, which in turn forms a curve; the filament motion deviating from the centerline of the plume is v_m, and the filament will be changed to be different shapes and sizes by small-scale vortex, expressed as v_d.
The position of a single molecule in motion can be expressed as:

$$p_m = v_a + v_m + v_d \quad (3)$$

The concentration at x = [x, y, z] at time t can be expressed as:

$$C(x, t) = \sum_i^N C_i(x, t)\frac{molecules}{cm^3} \quad (4)$$

The concentration produced by the filament i at coordinate x can be expressed as:

$$C_i(x, t) = \frac{Q}{\sqrt{8\pi^3 R_i^3(t)}} \exp\left(\frac{-r_i^2(t)}{-R_i^2(t)}\right)\frac{molecules}{cm^3 filament} \quad (5)$$

Where, Ri is the radius of the filament i; Pi(t) is the coordinate of the center position.

$$r_i(t) = \|x - p_i(t)\| cm \quad (6)$$

The puff radius is subjected to change with time, and the law is:

$$R(t) = (R(0) + \gamma t)^2 \quad (7)$$

R(0) and R(t) are the initial radius and the current radius of the filament, respectively. The gradient of the puff radius is shown as follow:

$$\frac{dR}{dt} = \frac{\gamma}{2R} \quad (8)$$

The dynamic model features obvious discontinuities of plume. It is widely It is therefore widely applied in outdoor simulation experiments with relatively complex environments (Muezzinoglu et al., 2009).

2.3 Plume discovery algorithm based on IoMT

For the unknown environment, the Spiral algorithm is mainly used to search for plume, and expressed as follows:

$$\begin{cases} x_r(k) = k \cdot a \cdot \omega \cdot \cos(k\omega) + x(0) \\ y_r(k) = k \cdot a \cdot \omega \cdot \sin(k\omega) + y(0) \end{cases} \quad (9)$$

Its motion trajectory mainly presents a spiral shape, which is controlled with given parameters k, a and w, as shown in Fig. 1.

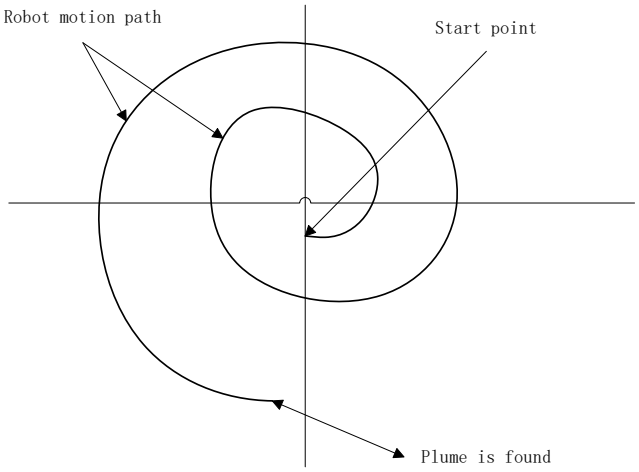

Figure 1: Spiral algorithm search smoke plume schematic

The schematic diagram of the trajectory of IoMT in the motion when the tracing the plume is shown in Fig. 2.

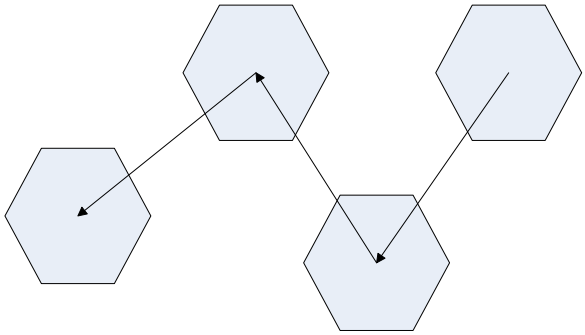

Figure 2: Traced smoke plume trajectories by mobile sensor array

3. Simulation experiment of odor source localization

In the odor source localization, this paper mainly uses the success rate and location error as the most important performance indicators. The layout of the sensor array presents a circle with a radius *r*, as shown in Fig. 3.

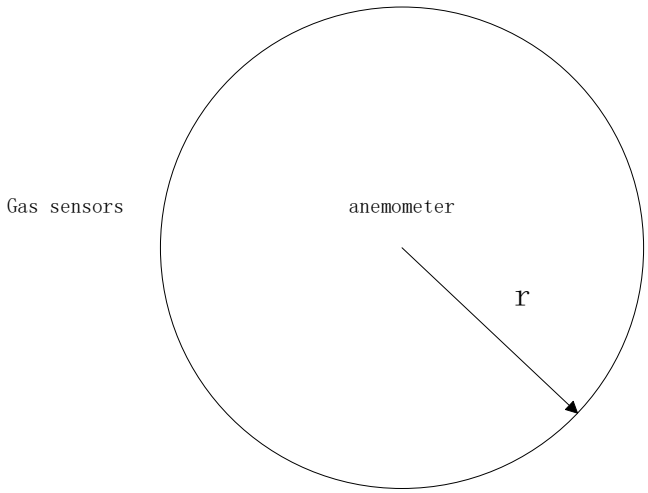

Figure 3: Traced smoke plume trajectories by mobile sensor array

In the simulation experiment of the outdoor environment, there are mainly three phases, namely Spiral search plume, LM algorithm plume trace and Spiral odor source declaration. In the indoor environment, the plume search is not required. Therefore, in the indoor simulation experiment, there are only two phases, i.e. the LM algorithm plume trace and the Spiral odor source declaration (Ding, 2018).
Before identifying the odor source, it is also required to determine whether the plume has been traced around the odor source. If this is the case, it will be able to preliminarily estimate the location of the odor source and stop tracing, otherwise, it continues to trace the plume. When searching for and tracing the plume, we need to continuously record and update the measured sensor coordinates (xmax, ymax) that correspond to the maximum concentrations, and then the *Spiral* verification algorithm can be performed, as shown in Fig.4.

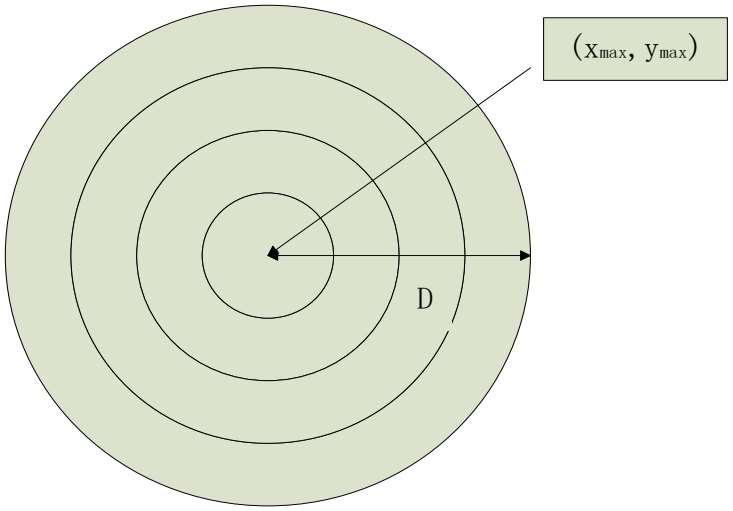

Figure 4: Spiral algorithm confirms the smell source

During indoor and outdoor simulation experiments, the focus is to explore what's effect the different step sizes and the distribution radius of the sensor will have on the localization of the odor source.
In the indoor simulation experiment, the step sizes for the plume trace are set to 10 cm, 20 cm, 30 cm, 40 cm, and 50 cm, respectively. The distribution radii *r* of the sensor are set to 0.1 m, 0.2 m, 0.3 m, 0.4 m and 0.5 m for simulation experiments, respectively. If the distance between the coordinate estimated at last and the odor source coordinate after odor source declaration does not exceed 0.5 m, it means that the odor source localization is successful. Simulation data of the location success rate and error accuracy under different combinations are shown in Table 1 and Table 2.

Table 1: The success rate of odor source localization under the indoor simulation environment

	10cm	20cm	30cm	40cm	50cm
10cm	85%	85%	100%	95%	85%
20cm	95%	95%	80%	100%	95%
30cm	95%	95%	100%	90%	95%
40cm	80%	95%	100%	100%	95%
50cm	95%	95%	100%	100%	95%

Table 2: Location error of odor source localization in indoor simulation environment (unit cm)

	10cm	20cm	30cm	40cm	50cm
10cm	5.3	6.8	4.9	7.2	9.9
20cm	5.3	6.7	4.2	5.6	9.3
30cm	8.5	6.7	5.9	10.3	10.6
40cm	7.2	5.6	9.7	7.5	10.5
50cm	6.7	5.4	7.8	8.4	15.7

Data in the tables 1 and 2 are the average values obtained from more than twenty simulation experiments. It is found from data listed in the table that the success rate of the indoor simulation experiment is much higher, and there is a fuzzy relationship between the step size, the sensor distribution radius and the odor source

localization. However, the success rate of odor source localization will be subjected to and decline if the distribution radii of step size and sensor get lesser. It is also found that the average localization error shows an upward trend as the sensor radius increases.

In the outdoor environment, attacked by the wind, the plume will change its movement direction, which affects the sensor's measurements on the concentration. The outdoor simulation results are shown in Tables 3 and 4. It is found from data in the table that, compared with the indoor simulation experiment, the success rate of the outdoor simulation is obviously lower. Like the indoor simulation experiment, there is also a tiny effect that step size and sensor distribution radius play on the success rate of outdoor simulation experiment, but when the step size falls within 250cm-400cm and the sensor distribution radius reaches 50cm or 60cm, the success rate of the simulation experiment gets higher. The success rate of simulation experiments is relatively high (Li and Fu, 2018). When the step value takes [100,500] and the sensor distribution radius falls within [30, 70], the odor source localization error does not depend on the specific values of the sensor distribution radius and the step size.

Table 3: The success rate of odor source localization in outdoor simulation environment

	30cm	40cm	50cm	60cm	70cm
100cm	65%	40%	75%	85%	60%
150cm	75%	60%	85%	80%	55%
200cm	65%	60%	95%	90%	30%
250cm	80%	65%	90%	100%	50%
300cm	60%	60%	100%	100%	20%
350cm	65%	50%	95%	90%	35%
400cm	85%	40%	100%	95%	40%
450cm	70%	80%	100%	100%	45%
500cm	75%	80%	90%	95%	30%

Table 4: Location error of odor source localization in outdoor simulation environment (unit cm)

	30cm	40cm	50cm	60cm	70cm
100cm	17.5	11.4	12.4	17.4	11.3
150cm	19.7	11.7	11.6	12.6	12.8
200cm	10.2	11.7	11.9	11.7	12.5
250cm	12.3	10.4	12.4	11.3	10.3
300cm	14.6	15.3	11.3	12.3	15.3
350cm	12.5	12.6	14.2	13.6	16.2
400cm	11.7	12.8	13.7	12.3	11.9
450cm	11.4	11.7	12.9	11.5	12.5
500cm	13.5	13.5	11.3	10.5	13.2

As described above, we can find that over high or too low step size and sensor distribution radius will lead the success rate of the simulation experiment to declining. Therefore, it is very important to select a reasonable range of values in the simulation experiment. In addition, the step size and the sensor distribution radius have a little effect on the error of the final odor source localization, and there is no obvious correlation between them.

4. Conclusion

Simulation experiment is conducted on the location of odor sources based on the IoMT in the indoor and outdoor environments, respectively. The results show that indoor simulation experiment has a very high success rate; there is a fuzzy relationship between the step size, the sensor distribution radius and the success rate of the odor source location, but too low step size and sensor distribution radius are lesser will have a certain negative effect on the success rate of the odor source location.

The success rate of the simulation experiment in outdoor environment is significantly lower than that in indoor environment. Step size and sensor distribution radius all have a little effect on the experimental success rate. however, when the step size falls within 250cm-400cm and the sensor distribution radius is 50cm or 60cm, the success rate of the simulation experiment gets higher.

When the step size and the sensor distribution radius are too high or too low, the success rate of the simulation experiment will decrease. Therefore, it is very important to select a reasonable range of values in the simulation experiment.

References

Agassounon W., Martinoli, A., Easton K., 2004, Macroscopic modeling of aggregation experiments using embodied agents in teams of constant and time-varying sizes, Autonomous Robots, 17(2-3), 163-192, DOI: 10.1023/b: auro.0000033971. 75494.c8

Ding X., 2018, Application of improved deep neural network in complex chemical soft measurement, Chemical Engineering Transactions, 66, 955-960, DOI: 10.3303/CET1866160

Esquivelzeta R.J., Mutlu K., Noutel J., Martin D.O.P., Haesler S., 2017, Spontaneous rapid odor source localization behavior requires interhemispheric communication, Current Biology, 27(10), 1542-1548, DOI: 10.1016/j.cub.2017.04.027

Frye M.A., Tarsitano M., Dickinson M.H., 2003, Odor localization requires visual feedback during free flight in drosophila melanogaster, Journal of Experimental Biology, 206(5), 843-855, DOI: 10.1242/jeb.00175

Gardiner, J. M., & Atema, J., 2007, Sharks need the lateral line to locate odor sources: rheotaxis and eddy chemotaxis, Journal of Experimental Biology, 210(11), 1925-1934, DOI: 10.1242/jeb.000075

Goken C., Gezici S., Arikan O., 2010, Optimal stochastic signaling for power-constrained binary communications systems, IEEE Transactions on Wireless Communications, 9(12), 3650-3661, DOI: 10.1109/twc.2010.101810.090902

Ishida H., Tanaka H., Taniguchi H., Moriizumi T., 2006, Mobile robot navigation using vision and olfaction to search for a gas/odor source, Autonomous Robots, 20(3), 231-238, DOI: 10.1007/s10514-006-7100-5

Kowadlo G., Russell R.A., 2006, Using naïve physics for odor localization in a cluttered indoor environment, Autonomous Robots, 20(3), 215-230, DOI: 10.1007/s10514-006-7102-3

Li J.G., Meng Q.H., Wang Y., Zeng M., 2011, Odor source localization using a mobile robot in outdoor airflow environments with a particle filter algorithm, Autonomous Robots, 30(3), 281-292, DOI: 10.1007/s10514-011-9219-2

Li M., Fu X., 2018, Molecular dynamics simulation of binary liquid mixture phase separation and glass transition, Chemical Engineering Transactions, 66, 229-234, DOI: 10.3303/CET1866039

Lu Q., Han Q. L., Xie X., Liu S., 2014, A finite-time motion control strategy for odor source localization, IEEE Transactions on Industrial Electronics, 61(10), 5419-5430, DOI: 10.1109/tie.2014.2301751

Lu Q., Liu S., Xie X., Wang J., 2013, Decision making and finite-time motion control for a group of robots, IEEE Transactions on Cybernetics, 43(2), 738-750, DOI: 10.1109/tsmcb.2012.2215318

Muezzinoglu M.K., Huerta R., Abarbanel H.D., Ryan M.A., Rabinovich M.I., 2009, Chemosensor-driven artificial antennal lobe transient dynamics enable fast recognition and working memory, Neural Computation, 21(21), 1018-1037, DOI: 10.1162/neco.2008.05-08-780

Pyk P., Badia S.B.I., Bernardet U., Knüsel P., Carlsson M., Gu J., 2006, An artificial moth: chemical source localization using a robot based neuronal model of moth optomotor anemotactic search, Autonomous Robots, 20(3), 197-213, DOI: 10.1007/s10514-006-7101-4

Sato K., Shu K., Kashiwadani H., Yamasoba T., Mori K., 2010, Spatial representation of odorant categories for the odor-source localization in the anterior olfactory nucleus pars externa, Neuroscience Research, 68, e385, DOI: 10.1016/j.neures.2010.07.1706

Saxena N., Natesan D., Sane S.P., 2018, Odor source localization in complex visual environments by fruit flies, Journal of Experimental Biology, 221(Pt 2), DOI: 10.1242/jeb.172023

Sumner J.H., 2006, Problems in odor research from the viewpoint of the chemistbasic odor research correlation, Annals of the New York Academy of Sciences, 58(2), 68-72, DOI: 10.1111/j.1749-6632. 1954.tb54845.x